OPEN BIOLOGY

royalsocietypublishing.org/journal/rsob

Research

Cite this article: Nerusheva OO, Ludzia P, Akiyoshi B. 2019 Identification of four unconventional kinetoplastid kinetochore proteins KKT22–25 in *Trypanosoma brucei*. *Open Biol.* **9**: 190236.
http://dx.doi.org/10.1098/rsob.190236

Received: 27 September 2019
Accepted: 7 November 2019

Subject Area:
biochemistry/cellular biology

Keywords:
kinetochore, kinetoplastid, *Trypanosoma brucei*, centromere, Gcn5-related *N*-acetyltransferase

Author for correspondence:
Bungo Akiyoshi
e-mail: bungo.akiyoshi@bioch.ox.ac.uk

Electronic supplementary material is available online at https://doi.org/10.6084/m9.figshare.c.4743647.

THE ROYAL SOCIETY PUBLISHING

Identification of four unconventional kinetoplastid kinetochore proteins KKT22–25 in *Trypanosoma brucei*

Olga O. Nerusheva, Patryk Ludzia and Bungo Akiyoshi

Department of Biochemistry, University of Oxford, Oxford OX1 3QU, UK

BA, 0000-0001-6010-394X

The kinetochore is a multi-protein complex that drives chromosome segregation in eukaryotes. It assembles onto centromere DNA and interacts with spindle microtubules during mitosis and meiosis. Although most eukaryotes have canonical kinetochore proteins, kinetochores of evolutionarily divergent kinetoplastid species consist of at least 20 unconventional kinetochore proteins (KKT1–20). In addition, 12 proteins (KKT-interacting proteins 1–12, KKIP1–12) are known to localize at kinetochore regions during mitosis. It remains unclear whether KKIP proteins interact with KKT proteins. Here, we report the identification of four additional kinetochore proteins, KKT22–25, in *Trypanosoma brucei*. KKT22 and KKT23 constitutively localize at kinetochores, while KKT24 and KKT25 localize from S phase to anaphase. KKT23 has a Gcn5-related *N*-acetyltransferase domain, which is not found in any kinetochore protein known to date. We also show that KKIP1 co-purifies with KKT proteins, but not with KKIP proteins. Finally, our affinity purification of KKIP2/3/4/6 identifies a number of proteins as their potential interaction partners, many of which are implicated in RNA binding or processing. These findings further support the idea that kinetoplastid kinetochores are unconventional.

1. Introduction

Kinetoplastids are a group of unicellular flagellated eukaryotes found in diverse environmental conditions [1]. It has been proposed that kinetoplastids may represent one of the earliest-branching eukaryotes based on a number of unique molecular features [2]. Understanding their biology could therefore provide insights into the extent of conservation or divergence among eukaryotes and lead to a deeper understanding of biological systems. Importantly, three neglected tropical diseases are caused by parasitic kinetoplastids: African trypanosomiasis, Chagas disease and leishmaniasis, caused by *Trypanosoma brucei*, *Trypanosoma cruzi* and *Leishmania* spp., respectively [3]. Although recent advances in public health and combination therapy have decreased the effect of these diseases, new drugs and druggable pathways are still very much needed against these diseases [4]. To this end, a more thorough understanding of the unique underlying biological mechanisms of kinetoplastids is critical.

One such fundamental process is the transmission of genetic material from mother to daughter cells, which is crucial for the survival of all organisms. Chromosome segregation in eukaryotes is driven by the kinetochore, a macromolecular protein complex that assembles onto centromeric DNA and captures spindle microtubules during mitosis [5]. Its structural core is typically composed of DNA-binding and microtubule-binding modules [6]. At least a fraction of core kinetochore proteins are present in nearly all sequenced eukaryotes, implying that most eukaryotes use a largely conserved mechanism of DNA and microtubule binding [7–9]. However, none of canonical kinetochore proteins have been identified in the genome of kinetoplastids [10,11]. To identify their kinetochore components, we previously carried out a YFP-tagging screen and identified a

protein that forms kinetochore-like dots [12]. Affinity purification of this protein identified co-purifying proteins whose localizations were subsequently examined by microscopy. This process was repeated until saturation, leading to the identification of 20 proteins that localize at kinetochores in *T. brucei*. Chromatin immunoprecipitation followed by deep sequencing confirmed that they are indeed kinetochore proteins, and we therefore named them KKT1–20 (kinetoplastid kinetochore proteins). Although these proteins are highly conserved among kinetoplastids, their apparent orthologues are absent in other eukaryotes, suggesting that kinetoplastids have an unconventional type of kinetochore proteins [12,13].

Recently, KKT-interacting protein 1 (KKIP1) was identified as a protein distantly related to Ndc80/Nuf2 microtubule-binding proteins based on weak similarity in the coiled-coil regions [14]. However, KKIP1 apparently lacks the calponin homology (CH) domain, a critical feature of Ndc80/Nuf2 proteins. KKIP1 therefore does not appear to be a genuine Ndc80/Nuf2 orthologue. Nonetheless, KKIP1 localizes at kinetochores and its depletion causes severe chromosome segregation defects [14]. Immunoprecipitation of KKIP1 from chemically cross-linked cells led to the identification of six additional proteins (KKIP2–7) that localize to kinetochore regions during mitosis [14]. Very recently, immunoprecipitation of KKIP2–7 from non-cross-linked cells identified a nine-subunit protein complex called the KOK (kinetoplastid outer kinetochore) complex that consists of KKIP2, 3, 4, 6, 8, 9, 10, 11 and 12 [15]. KKT proteins were not detected in the immunoprecipitates of KKIP2–12 or KKIP1 without chemical cross-linking [15]. It therefore remains unclear whether KKIP1–12 interact with KKT proteins in native conditions.

A hallmark of kinetochores in most eukaryotes is the presence of specialized nucleosomes containing the centromere-specific histone H3 variant CENP-A, which epigenetically specifies the position of kinetochore assembly, forms the primary anchorage point to DNA and recruits other kinetochore proteins [16]. However, CENP-A is absent in kinetoplastids. It therefore remains unknown how their kinetochores assemble specifically at centromeres. *Trypanosoma brucei* has 11 large chromosomes that have regional centromeres of 20–120 kb in size, as well as approximately 100 small chromosomes that lack centromeres [17–19]. Although kinetochore assembly sites on large chromosomes are apparently determined in a sequence-independent manner, the underlying mechanism remains a mystery.

To understand how unconventional kinetoplastid kinetochores perform conserved functions such as kinetochore specification, it is critical to have a complete constituent list. In this study, we report the identification of four additional kinetochore proteins in *T. brucei*.

2. Results

2.1. Identification of KKT22 and KKT23 in *Trypanosoma brucei*

Our previous immunoprecipitation of KKT3 that was N-terminally tagged with YFP (YFP-KKT3) did not result in co-purification of other kinetochore proteins [12]. To verify this result, we made a strain that had a C-terminally YFP-tagged KKT3 (KKT3-YFP) as the sole copy of KKT3 and performed its immunoprecipitation using the same protocol. We detected a number of kinetochore proteins by mass spectrometry (figure 1*a*; electronic supplementary material, table S1), suggesting that YFP-KKT3 was not fully functional. In addition to known kinetochore proteins, there were two uncharacterized proteins (ORF Tb927.9.6420 and Tb927.10.6600) that co-purified with KKT3-YFP in an apparently specific manner (figure 1*a*). We tagged these proteins with an N-terminal YFP at the endogenous locus and found that they localized at kinetochores throughout the cell cycle (figure 1*b*,c). Immunoprecipitation of these proteins showed that they specifically co-purified with other KKT proteins (figure 1*d*,*e*). We therefore named them KKT22 and KKT23. These proteins were not detected in the immunoprecipitates of any other kinetochore protein [12], so it is likely that these proteins are closely associated with KKT3.

Homology search of KKT22 identified apparent orthologues in several kinetoplastids (table 1), but not in *Bodo saltans* (a free-living kinetoplastid) or other eukaryotes. A profile–profile comparison using HHpred [20] did not reveal any obvious domain, except for a possible zinc hook motif of Rad50 (electronic supplementary material, figure S1). KKT23 has a Gcn5-related *N*-acetyltransferase (GNAT) domain [21–23], which is not found in any known kinetochore protein in other eukaryotes. In humans, TIP60 and KAT7/HBO1/MYST2 acetyltransferases (both are members of the MYST subfamily) are known to regulate kinetochore functions but are not part of core kinetochores [24,25]. We found that KKT23 co-purified with many KKT proteins (figure 1*e*), implying that it is a core kinetochore protein in *T. brucei*. Interestingly, our sequence analysis failed to identify an obvious orthologous relationship with known GNAT subfamily members, suggesting that KKT23 forms a distinct subfamily. Our finding that an apparent orthologue of KKT23 is found even in divergent kinetoplastids (*B. saltans* and *Perkinsela*; table 1; electronic supplementary material, figure S2) raises a possibility that it plays a fundamental role at the kinetoplastid kinetochore, which warrants further investigation.

2.2. Identification of KKT24

In our purification of YFP-KKT22, there was another kinetochore protein candidate (ORF Tb927.10.4200; figure 1*d*). We found that this protein, in fact, localized at kinetochores from S phase to anaphase (figure 2*a*) and its immunoprecipitation confirmed specific co-purification with other kinetochore proteins (figure 2*b*). We therefore named it KKT24. Interestingly, KKT24 and KKIP1 share several similarities. Both proteins are predicted to consist mostly of coiled coils (electronic supplementary material, figure S3) [14], and their N-termini are located at the outer region of kinetochores, as judged by the formation of pairs of dots in metaphase (figure 2*a*) [15,26]. However, our immunoprecipitation data do not support a possibility that KKT24 and KKIP1 form a stable complex (figure 2*b* and see below). We also note that obvious orthologues for KKT24 and KKIP1 are not found in free-living *B. saltans*, an organism that has essentially all of KKT1–20 proteins (table 1) [12,13].

2.3. Identification of KKT25

Our purification of KKT24 led to the identification of another kinetochore protein candidate (ORF Tb927.8.2830) (figure 2*b*), which indeed localized at kinetochores from S phase to anaphase (figure 3*a*). We confirmed that this protein co-purified

(*a*)

proteins co-purified with KKT3-YFP	Mascot score	no. peptides	coverage (%)
KKT3	4112	194	49.6
KKT2	1096	39	35.9
KKT7	961	43	52.0
KKT1	788	32	19.9
KKT8	395	12	37.3
KKT9	208	8	24.3
KKT10	188	7	18.9
KKT6	175	13	33.7
KKT4	133	6	21.2
KKT19	132	6	20.5
KKT14	127	4	14.2
Tb927.9.6420 (KKT22)	119	6	33.9
Tb927.10.6600 (KKT23)	105	7	33.3
KKT11	101	4	21.9

(*b*)

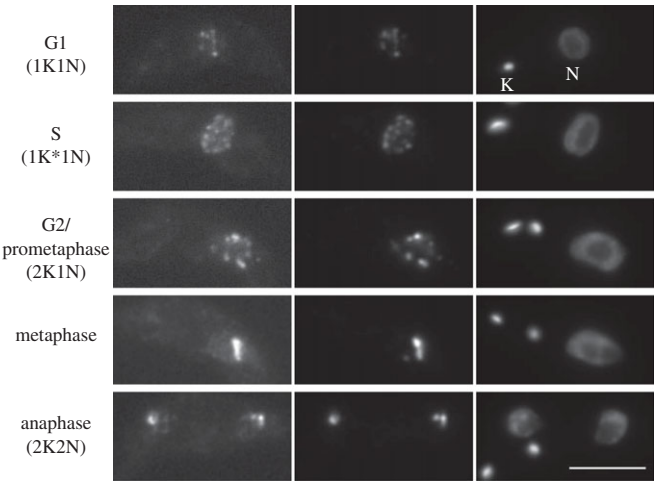

(*c*)

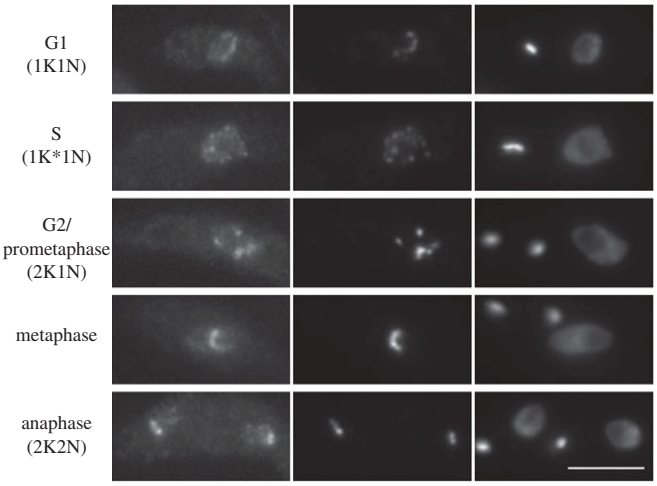

(*d*)

proteins co-purified with YFP-KKT22	Mascot score	no. peptides	coverage (%)
KKT3	9597	426	38.2
KKT7	7351	273	49.1
KKT1	4377	124	15.0
KKT8	3940	103	34.8
KKT2	3553	104	22.1
KKT4	1595	40	19.8
KKT6	1489	42	25.9
KKT23	1045	38	7.8
KKT10	999	46	16.8
KKT14	815	39	16.2
KKT5	640	23	15.4
KKT9	579	35	32.2
KKT19	533	26	22.1
KKT12	394	11	15.0
Tb927.10.4200 (KKT24)	178	11	6.0
KKT22	85	10	15.8

(*e*)

proteins co-purified with YFP-KKT23	Mascot score	no. peptides	coverage (%)
KKT3	5560	258	39.3
KKT7	1775	62	37.9
KKT22	1480	67	45.1
KKT1	897	30	16.3
KKT8	864	24	41.9
KKT2	756	21	15.6
KKT4	708	13	15.8
KKT6	386	9	30.7
KKT23	345	12	37.4
KKT9	329	16	31.3
KKT19	295	8	32.6
KKT14	207	6	20.7
KKT10	201	7	15.7
KKT5	201	5	21.1
KKT11	101	3	12.0
KKT12	95	2	14.5

Figure 1. Identification of KKT22 and KKT23. (*a*) KKT3-YFP co-purifies with a number of KKT proteins, including two kinetochore protein candidates, KKT22 and KKT23. See electronic supplementary material, table S1 for all proteins identified by mass spectrometry. Cell line, BAP1123. (*b*) YFP-KKT22 and (*c*) YFP-KKT23 localize at kinetochores throughout the cell cycle. K and N represent the kinetoplast (mitochondrial DNA) and nucleus, respectively. These organelles have distinct replication and segregation timings and serve as good cell-cycle markers. K* is an elongated kinetoplast and indicates that the nucleus is in S phase. Fluorescent protein signals were directly detected by microscopy. Similar results were obtained with KKT22-YFP and KKT23-YFP (data not shown). Bars, 5 µm. BAP1454 and BAP1593. (*d*) KKT22 co-purifies with KKT proteins and another kinetochore protein candidate, KKT24. BAP1490. (*e*) KKT23 co-purifies with KKT proteins. BAP1549.

with various kinetochore proteins (figure 3*b*) and therefore named it KKT25. Like KKT22 and KKT24, it is conserved in many kinetoplastids, but not in *B. saltans* or other eukaryotes (table 1; electronic supplementary material, figure S4). We failed to identify any obvious domain or predicted coiled coils in KKT25.

2.4. KKIP1 co-purifies with KKT proteins, not with KKIP proteins

A previous study by D'Archivio & Wickstead [14] identified a putative kinetochore protein KKIP1 that localized to kinetochores. Its immunoprecipitation from chemically cross-linked

Table 1. Conservation of KKT22–25, KKIP1 and KKIP5 among kinetoplastids.

	KKT22	KKT23	KKT24	KKT25	KKIP1	KKIP5
T. brucei	Tb927.9.6420	Tb927.10.6600	Tb927.10.4200	Tb927.8.2830	Tb927.5.4520	Tb927.7.6630
T. congolense		TcIL3000_10_5670	TcIL3000_10_3510	TcIL3000_0_41350	TcIL3000_5_5210	TcIL3000_0_33690
T. grayi	DQ04_05731010	DQ04_07341010	DQ04_12781000	DQ04_02041070	DQ04_01751000	DQ04_10231010
T. vivax		TvY486_1006570	TvY486_0019400	TvY486_0802340	TvY486_0503940	TvY486_0706450
T. cruzi	TcCLB.506509.60	TcCLB.510187.340	TcCLB.511467.50	TcCLB.504427.170	TcCLB.509539.40	TcCLB.510055.70
T. rangeli	TRSC58_06150		TraAM80_06991	TRSC58_01409	TRSC58_03083	TRSC58_00449
T. theileri	TM35_000182020	TM35_000022840	TM35_000421720	TM35_000132550	TM35_000061590	TM35_000202190
Blechomonas	Baya_113_0090	Baya_001_0150	Baya_039_0490	Baya_024_0050	Baya_086_0290	Baya_072_0080
Crithidia		CFAC1_250031900	CFAC1_240027400	CFAC1_150014500	CFAC1_020006200	CFAC1_090010600
Leptomonas		Lsey_0046_0080	Lsey_0122_0130	Lsey_0053_0040	Lsey_0120_0220	Lsey_0154_0070
Endotrypanum		EMOLV88_360026200	EMOLV88_350006300	EMOLV88_230010500	EMOLV88_050005000	EMOLV88_170008400
L. mexicana	LmxM.15.0825	LmxM.36.2100	LmxM.34.0180	LmxM.23.1610	LmxM.05.0010	LmxM.17.0430
Phytomonas	GSEM1_T00007051001	GSEM1_T00000676001	GSEM1_T00004838001	GSEM1_T00006110001	GSEM1_T00003924001	GSEM1_T00002551001
Paratrypanosoma	PCON_0021420	PCON_0016010	PCON_0019770	PCON_0076260	PCON_0068010	
B. saltans		BSAL_82255				
Perkinsela		XU18_2502				

(*a*)

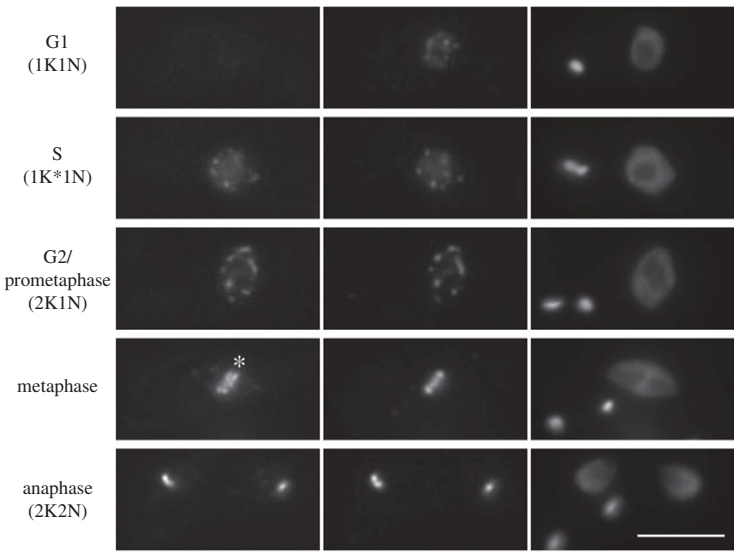

(*b*)

proteins co-purified with YFP-KKT24	Mascot score	no. peptides	coverage (%)
KKT7	4400	153	69.3
KKT24	4191	126	60.2
KKT1	3024	106	27.5
KKT2	2735	88	38.7
KKT9	2495	88	78.4
KKT8	1913	52	73.2
KKT4	1556	33	46.8
KKT14	1098	29	31.5
KKT10	908	40	37.2
KKT19	724	34	36.0
KKT11	688	24	49.0
Tb927.8.2830 (KKT25)	684	32	42.2
KKT6	565	20	45.4
KKT5	481	19	34.2
KKIP5	377	7	16.9
KKT3	302	12	17.6

Figure 2. Identification of KKT24. (*a*) KKT24 localizes at kinetochores from S phase to anaphase. Note that YFP-KKT24 signals appear as pairs of dots (indicated by asterisk). Fluorescent protein signals were directly detected by microscopy. Bar, 5 µm. Cell line, BAP1819. (*b*) KKT24 co-purifies with a number of KKT proteins, KKIP5, and another kinetochore protein candidate, KKT25. BAP1635.

(*a*)

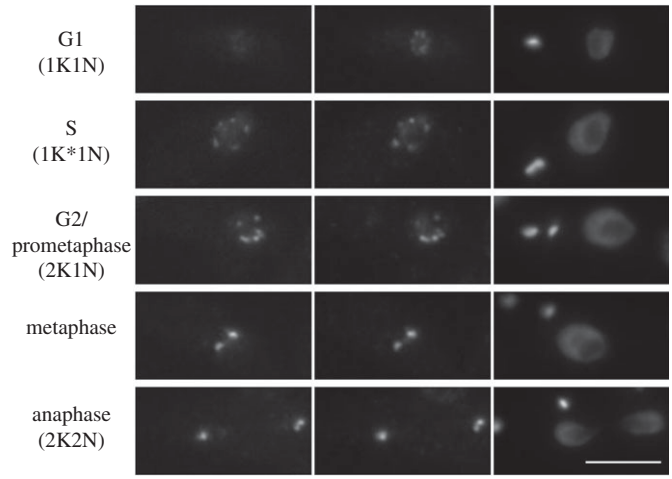

(*b*)

proteins co-purified with YFP-KKT25	Mascot score	no. peptides	coverage (%)
KKT24	8496	277	50.5
KKT7	1123	48	32.8
KKT25	881	28	49.4
KKT8	531	16	29.1
KKT2	420	14	13.0
KKT1	404	19	20.6
KKT4	387	8	13.0
KKIP5	386	11	13.5
KKT14	265	8	13.3
KKT6	181	6	25.9
KKT9	175	11	37.1
KKT19	145	4	16.1
KKT5	129	5	25.4
KKT12	123	3	14.5

Figure 3. Identification of KKT25. (*a*) YFP-KKT25 localizes at kinetochores from S phase to anaphase. Fluorescent protein signals were directly detected by microscopy. Bar, 5 µm. Cell line, BAP1820. (*b*) KKT25 co-purifies with a number of KKT proteins and KKIP5. BAP1742.

trypanosome cells led to co-purification of many nuclear proteins including KKT proteins and KKIP2–7 [14]. However, KKT proteins were not detected in the KKIP1 immunoprecipitate without cross-linking [15], so the relationship between KKIP1 and KKT proteins remained unclear. While re-searching our previous mass spectrometry data [12] against a newer version of the *T. brucei* proteome database, we found that KKIP1 was actually present in the immunoprecipitate of KKT2 (figure 4*a*). We had therefore named it KKT21 but switched to use the name KKIP1 following the publication of the D'Archivio & Wickstead paper. Immunoprecipitation of KKIP1 using our protocol revealed co-purification with a number of KKT proteins (figure 4*b*), showing that KKIP1 is a genuine kinetochore protein. It is important to mention that we did not detect KKIP2–7 in our KKIP1 immunoprecipitation sample. This raises a possibility that previous identification of KKIP2–7 in the immunoprecipitate of KKIP1 from cross-linked cells was due to the artificial chemical cross-linking, which is consistent with the identification of many nuclear proteins in the same sample [14].

2.5. KOK subunits co-purify with a number of proteins with RNA-related functions

Immunoprecipitation of KKIP2–7 from non-cross-linked cells identified a complex called the KOK complex that consists of nine KKIP proteins (KKIP2, 3, 4, 6, 8, 9, 10, 11 and 12) and localizes at the outer region of kinetochores during mitosis [15]. It has been proposed that KKIP1 provides a linkage between inner kinetochores and the KOK complex, despite the fact that KKIP1 was not detected in the immunoprecipitates of any KOK components [15]. To reveal the relationship between the KOK complex and KKT proteins, we performed immunoprecipitation of KKIP2–7 using our purification protocol. Immunoprecipitation of KKIP7 did not reveal any specific interacting proteins (electronic supplementary material, table S1), while that of KKIP5 was unsuccessful despite multiple attempts (electronic supplementary material, table S1; additional data not shown). By contrast, immunoprecipitation of KKIP2, KKIP3, KKIP4 and KKIP6 revealed a number of co-purifying proteins, including the KOK components

(*a*)

proteins co-purified with YFP-KKT2	Mascot score	no. peptides	coverage (%)
KKT2	1773	55	46.0
KKT1	1023	31	23.5
KKT7	701	22	45.5
KKT8	538	17	59.6
KKT11	302	8	32.3
KKT10	295	13	27.7
KKT16	291	4	43.3
KKT9	287	9	32.2
KKT6	238	6	28.3
KKIP1	219	6	16.2
KKT4	173	3	11.5
KKT14	156	3	10.4
KKT17	138	4	17.2
KKT19	129	8	22.7
KKT15	127	2	22.8

(*b*)

proteins co-purified with YFP-KKIP1	Mascot score	no. peptides	coverage (%)
KKT1	4022	172	33.5
KKT7	3824	176	78.9
KKIP1	3607	182	61.3
KKT9	2765	98	75.1
KKT8	2216	81	80.7
KKT2	1626	79	48.1
KKT4	1529	58	54.9
KKT14	710	28	46.3
KKT6	641	24	42.4
KKT11	614	32	62.9
KKT10	448	25	33.5
KKT19	440	23	35.7
KKT5	404	23	40.4
KKT15	301	14	33.4
KKT3	203	18	17.9

Figure 4. KKIP1 co-purifies with KKT proteins, not with KKIP proteins. (*a*) Re-analysis of our previous mass spectrometry data [12] identifies KKIP1 in the KKT2 immunoprecipitate. (*b*) YFP-KKIP1 co-purifies with a number of KKT proteins but with none of other KKIP proteins. Cell line, BAP710.

(figure 5*a–d*). Besides Tb927.3.3740 and Tb927.2.3160/Gar1, which were detected in the previous report [15], 10 additional proteins were identified as apparent interactors of KKIP2/3/4/6, many of which have putative domains implicated in RNA binding, transcription or splicing (figure 5*e*). Interestingly, our HHpred analysis also revealed a similarity to a CTD kinase subunit in KKIP6 as well as a putative RNA recognition motif in KKIP4, KKIP9 and KKIP10 (figure 5*e*). The functional significance of these factors for kinetochore functions, if any, remains to be determined. Although we did not detect significant amounts of KOK components in our immunoprecipitates of KKT proteins or KKIP1, several kinetochore proteins were detected in the immunoprecipitates of KOK components, especially KKIP3 (figure 5*b*). Because KKIP1 did not co-purify with any KOK components using the same purification protocol (figure 4*b*), kinetochore localization of the KOK complex may be mediated by KKIP3, rather than KKIP1.

3. Discussion

In this study, we identified four additional kinetochore components in *T. brucei* (KKT22–25). We also confirmed that KKIP1 is a genuine kinetochore protein. It is possible that KKIP5 is also a kinetochore protein based on its presence in the immunoprecipitates of KKT24 and KKT25 (figures 2*b* and 3*b*) as well as observed chromosome segregation defects upon depletion of KKIP5 [27]. Our original definition of genuine kinetochore proteins in *T. brucei* was that any such protein should co-purify 'only' with other kinetochore proteins (except for KKT4 and KKT20 that also co-purify with APC/C subunits) [12,13]. According to this definition, components of the KOK complex are not genuine kinetochore proteins because they co-purify with a number of factors that are implicated in RNA binding or processing. However, it has been clearly shown that KOK components localize at outer kinetochore regions at least during metaphase [14,15]. More importantly, our immunoprecipitation of KKIP3 revealed co-purification with several KKT proteins, suggesting that the KOK complex indeed localizes at kinetochores. Defects in chromosome segregation have not been reported after knockdown of KOK components or its interaction partners [15]. We speculate that the KOK complex might be involved in the segregation of small chromosomes, rather than large chromosomes, in *T. brucei*.

The identification of a kinetochore protein that has a GNAT domain reinforces the idea that kinetoplastid kinetochores are unconventional. It will be important to test whether the GNAT domain of KKT23 is important for kinetochore functions. Acetylation of unknown substrates (possibly histones or kinetochore proteins) at centromeres might mark the position of kinetochore assembly sites in kinetoplastids that lack CENP-A. It is noteworthy that the genome-wide tagging project in *T. brucei* has come to an end, and did not identify any additional kinetochore components [28,29]. It is possible that we now have a complete list of kinetochore components, which include KKT1–20, KKIP1 and KKT22–25 (figure 6). Characterization of their functions and structures is not only important for our better understanding of eukaryotic chromosome segregation machinery but also for the development of new drugs against kinetoplastid diseases.

4. Material and methods

4.1. Cells

All cell lines, plasmids and primers/synthetic DNA used in this study are listed in electronic supplementary material, tables S2, S3 and S4, respectively. All cell lines used in this study were derived from *T. brucei* SmOxP927 procyclic form cells (TREU 927/4 expressing T7 RNA polymerase and the tetracycline repressor to allow inducible expression) [32]. Cells were grown at 28°C in SDM-79 medium supplemented with 10% (v/v) heat-inactivated fetal calf serum [33]. The cell line carrying KKT3-YFP as the sole copy of KKT3 was made by deleting one allele of KKT3 by a fusion PCR method [34] using a neomycin gene cassette from pBA183, followed by tagging of the remaining allele with a C-terminal YFP using a PCR-based method with a blasticidin selection marker [35]. N-terminally YFP-tagged KKT22 was made by a PCR-based method using pPOTv7 (eYFP, blasticidin) [35]. Endogenous YFP tagging for KKT23–25 and KKIP1–7 was performed using the pEnT5-Y vector [36] with PCR products or synthesized DNA fragments using XbaI/BamHI sites. Endogenous tdTomato tagging of

(*a*)

proteins co-purified with YFP-KKIP2	Mascot score	no. peptides	coverage (%)
KKIP3	5752	270	85.8
KKIP11	3596	164	64.3
KKIP2	2157	71	30.0
KKIP8	1625	72	40.5
KKIP9	460	14	37.2
KKIP10	258	12	37.3
KKIP4	254	12	38.0
KKIP6	204	4	8.2
KKIP12	132	4	42.8
Tb927.10.11600	90	3	12.4
Tb927.3.3740	76	2	10.0
KKT1	71	5	7.8
KKT7	62	3	12.3

(*b*)

proteins co-purified with YFP-KKIP3	Mascot score	no. peptides	coverage (%)
KKIP3	3357	157	78.5
KKIP11	3222	142	66.5
KKIP2	1571	44	26.8
KKT1	880	27	23.3
KKIP8	855	37	31.6
KKT2	684	21	30.2
KKT7	615	34	53.7
KKT4	458	16	40.8
KKIP9	456	16	34.5
KKIP4	316	17	35.7
KKIP10	312	12	32.4
KKT14	257	10	20.0
Tb927.10.11600	231	8	20.2
KKIP6	164	4	15.1
Tb927.3.3740	164	7	28.7
KKT6	152	3	29.3
Tb927.7.5590	136	4	11.6
KKT24	118	5	13.2
KKIP12	118	2	15.6

(*c*)

proteins co-purified with YFP-KKIP4	Mascot score	no. peptides	coverage (%)
KKIP4	9534	367	72.3
KKIP9	8129	291	71.7
KKIP10	6115	292	68.2
Tb927.3.3740	5233	231	85.0
Tb927.10.11600	4158	184	58.4
KKIP12	4141	143	80.4
Tb927.7.5590	3609	164	35.3
KKIP6	3536	145	64.0
Tb927.11.7450	2078	96	55.4
Tb927.11.2900	1596	45	77.8
Tb927.2.3160	757	29	43.6
Tb927.8.7400	592	30	20.0
Tb927.10.170	591	28	47.3
Tb927.5.3250	577	21	18.1
Tb927.7.6320	522	15	20.8
KKIP11	489	20	26.1
KKIP8	489	13	20.9
KKIP3	408	22	40.9
Tb927.10.4740	330	17	87.3

(*d*)

proteins co-purified with YFP-KKIP6	Mascot score	no. peptides	coverage (%)
KKIP9	6003	172	76.7
KKIP4	5933	218	76.0
KKIP10	5825	216	65.3
KKIP12	3551	85	82.4
Tb927.7.5590	2120	82	30.5
Tb927.10.11600	1941	77	54.4
Tb927.3.3740	1783	106	79.4
KKIP6	1780	57	55.6
Tb927.11.7450	588	26	30.1
Tb927.5.3250	586	18	20.7
Tb927.11.2900	584	18	60.8
Tb927.4.5020	555	20	16.5
Tb927.10.170	529	19	42.4
KKIP3	497	23	40.7
KKIP11	483	20	30.9
Tb927.10.4740	310	14	87.3

(*e*)

name	annotation and domains
Tb927.10.11600	**putative splicing factor, arginine/serine-rich domain**
Tb927.3.3740	**zinc-finger double-stranded RNA-binding**
Tb927.7.5590	domain of unknown function (DUF3883)
Tb927.11.7450	HIT zinc finger
Tb927.11.2900	HIT zinc finger
Tb927.2.3160	**H/ACA ribonucleoprotein complex subunit, Gar1/Naf1 RNA binding region**
Tb927.10.4740	**H/ACA ribonucleoprotein complex subunit Nop10**
Tb927.10.170	**H/ACA ribonucleoprotein complex subunit Cbf5, tRNA pseudouridine synthase**
Tb927.5.3250	**weak similarity to pre-mRNA-splicing factor 8**
Tb927.7.6320	BTB/POZ domain, regulator of chromosome condensation (RCC1) repeat
Tb927.8.7400	**RNA polymerase IIA largest subunit**
Tb927.4.5020	**DNA-directed RNA polymerase II subunit RPB1**
KKIP2	hypothetical protein
KKIP3	putative PDZ domain
KKIP4	**putative RNA recognition motif (RRM)**
KKIP6	**weak similarity to CTD kinase subunit gamma**
KKIP8	**poly(A) polymerase**
KKIP9	**putative RNA recognition motif (RRM)**
KKIP10	**putative RNA recognition motif (RRM)**
KKIP11	hypothetical protein
KKIP12	**RBP34, RNA-binding protein, putative RNA recognition motif (RRM)**

Figure 5. KOK subunits co-purify with a number of proteins with RNA-related functions. (*a–d*) Mass spectrometry summary tables of KKIP2, KKIP3, KKIP4 and KKIP6 immunoprecipitates. Cell lines, BAP825, BAP826, BAP808 and BAP828. (*e*) Putative domains in the identified proteins and KOK subunits.

KKT2 was performed using pBA164 that has a blasticidin selection marker [13] or pBA809 that has a neomycin marker. pBA809 was made by subcloning of the KKT2 targeting fragment from pBA67 [12] into pEnT6-tdTomato [36] using XbaI/BamHI sites. All constructs were sequence verified. Plasmids linearized by NotI were transfected to trypanosomes by

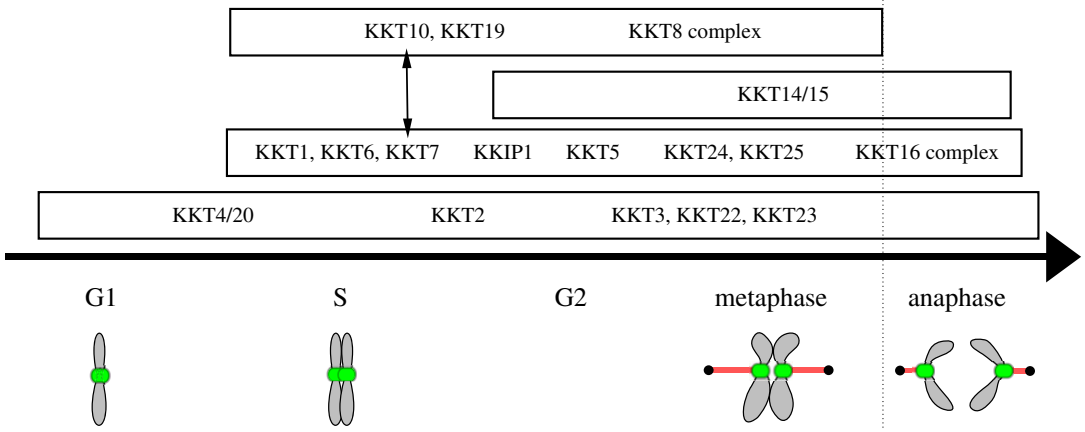

Figure 6. Localization patterns of kinetoplastid kinetochore proteins. Note that direct protein–protein interactions have not been established for many kinetochore proteins, except for the KKT7–KKT10 interaction (indicated by two-headed arrow) and the KKT8 complex that consists of KKT8, KKT9, KKT11 and KKT12 [30]. The putative KKT16 complex consists of KKT16, KKT17 and KKT18 [12]. S-phase-specific kinetochore protein KKT13 is not shown. Modified from [12,31] under the Creative Commons Attribution License.

electroporation into an endogenous locus. Transfected cells were selected by the addition of 25 µg ml^{-1} hygromycin (pEnT5-Y derivatives), 10 µg ml^{-1} blasticidin (pBA164 or pPOTv7-based PCR products) or 30 µg ml^{-1} G418 (pBA809 or pBA183-based PCR products).

4.2. Fluorescence microscopy

Cells were fixed with 4% paraformaldehyde for 5 min and images were captured at room temperature on a DeltaVision fluorescence microscope (Applied Precision) installed with softWoRx v.5.5 housed in the Micron Oxford essentially as described [13] using 100× objective lenses (1.42 NA). Images were processed in ImageJ [37]. We confirmed that there was no notable bleed-through signal from different channels in our experiments. Typically, 12 optical slices spaced 0.25 µm apart were collected, and single plane images are shown. Figures were made using Inkscape (The Inkscape Team) and converted to the EPS format.

4.3. Immunoprecipitation and mass spectrometry

Immunoprecipitation was performed as previously described using mouse monoclonal anti-GFP antibodies (Roche, 11814460001) that had been pre-conjugated with Protein G magnetic beads (Thermo Fisher Scientific, 10004D) with dimethyl pimelimidate (Sigma, D8388) [12]. Mass spectrometry was also performed essentially as previously described using a Q Exactive (Thermo Scientific) at the Advanced Proteomics Facility, University of Oxford [12]. Peptides were identified by Mascot (Matrix Science) using a custom *T. brucei* proteome database that contains predicted proteins in TriTrypDB (v.4) [38] supplemented with predicted small proteins [39,40]. Proteins identified with at least two peptides were considered as significant and shown in electronic supplementary material, table S1.

4.4. Bioinformatics

Search for homologous proteins were done using BLAST in TriTrypDB [38,41], Jackhmmer on the UniProtKB proteome database using a default setting (HmmerWeb v.2.39 [42]) or hmmsearch on select proteomes using manually prepared hmm profiles (HMMER v.3.0 [43]). A protein with the best score in a given species was considered as a putative orthologue if a reciprocal search using BLAST or Jackhmmer identified the starting query protein as the best hit in the original species. HHpred was carried out using pfamA_v32.0 and PDB_mmCIF70 databases [20]. The multiple sequence alignment was performed with MAFFT (L-INS-i method, v.7) [44] and visualized with the Clustalx colouring scheme in Jalview (v.2.10) [45]. Coiled coils were predicted using COILS [46]. Accession numbers for protein sequences were retrieved from TriTrypDB [11,38,47–51] or UniProt [52].

Data accessibility. All data are available upon request.

Authors' contributions. O.O.N. performed immunoprecipitation of KKT3 and KKIP1–7, and identified KKT22 and KKT23. B.A. performed immunoprecipitation of KKT22, KKT23 and KKT25, and identified KKT24. P.L. performed immunoprecipitation of KKT24 and identified KKT25. All authors participated in data analysis. B.A. wrote the manuscript. All authors gave final approval for publication and agreed to be held accountable for the work performed therein.

Competing interests. We declare we have no competing interests.

Funding. P.L. was supported by Boehringer Ingelheim Fonds. B.A. was supported by a Wellcome Trust Senior Research Fellowship (grant no. 210622/Z/18/Z) and the European Molecular Biology Organization Young Investigator Program.

Acknowledgements. We thank Midori Ishii for comments on the manuscript and the Advanced Proteomics Facility, especially Svenja Hester and Sabrina Liberatori, for mass spectrometry analysis, as well as Micron Oxford. We also thank Samuel Dean for providing pPOT plasmids.

References

1. d'Avila-Levy CM *et al.* 2015 Exploring the environmental diversity of kinetoplastid flagellates in the high-throughput DNA sequencing era. *Mem. Inst. Oswaldo Cruz* **110**, 956–965. (doi:10.1590/0074-0276150253)
2. Cavalier-Smith T. 2010 Kingdoms Protozoa and Chromista and the eozoan root of the eukaryotic

tree. *Biol. Lett.* **6**, 342–345. (doi:10.1098/rsbl.2009.0948)

3. Stuart K, Brun R, Croft S, Fairlamb A, Gürtler RE, McKerrow J, Reed S, Tarleton R. 2008 Kinetoplastids: related protozoan pathogens, different diseases. *J. Clin. Invest.* **118**, 1301–1310. (doi:10.1172/JCI33945)
4. Field MC *et al*. 2017 Anti-trypanosomatid drug discovery: an ongoing challenge and a continuing need. *Nat. Rev. Microbiol.* **15**, 447. (doi:10.1038/nrmicro.2017.69)
5. McIntosh JR. 2016 Mitosis. *Cold Spring Harb. Perspect. Biol.* **8**, a023218. (doi:10.1101/cshperspect.a023218)
6. Musacchio A, Desai A. 2017 A molecular view of kinetochore assembly and function. *Biology* **6**, 5. (doi:10.3390/biology6010005)
7. Meraldi P, McAinsh AD, Rheinbay E, Sorger PK. 2006 Phylogenetic and structural analysis of centromeric DNA and kinetochore proteins. *Genome Biol.* **7**, R23. (doi:10.1186/gb-2006-7-3-r23)
8. Drinnenberg IA, Akiyoshi B. 2017 Evolutionary lessons from species with unique kinetochores. *Prog. Mol. Subcell. Biol.* **56**, 111–138. (doi:10.1007/978-3-319-58592-5_5)
9. van Hooff JJ, Tromer E, van Wijk LM, Snel B, Kops GJ. 2017 Evolutionary dynamics of the kinetochore network in eukaryotes as revealed by comparative genomics. *EMBO Rep.* **18**, 1559–1571. (doi:10.15252/embr.201744102)
10. Lowell JE, Cross GAM. 2004 A variant histone H3 is enriched at telomeres in *Trypanosoma brucei*. *J. Cell. Sci.* **117**, 5937–5947. (doi:10.1242/jcs.01515)
11. Berriman M *et al*. 2005 The genome of the African trypanosome *Trypanosoma brucei*. *Science* **309**, 416–422. (doi:10.1126/science.1112642)
12. Akiyoshi B, Gull K. 2014 Discovery of unconventional kinetochores in kinetoplastids. *Cell* **156**, 1247–1258. (doi:10.1016/j.cell.2014.01.049)
13. Nerusheva OO, Akiyoshi B. 2016 Divergent polo box domains underpin the unique kinetoplastid kinetochore. *Open Biol.* **6**, 150206. (doi:10.1098/rsob.150206)
14. D'Archivio S, Wickstead B. 2017 Trypanosome outer kinetochore proteins suggest conservation of chromosome segregation machinery across eukaryotes. *J. Cell Biol.* **216**, 379–391. (doi:10.1083/jcb.201608043)
15. Brusini L, D'Archivio S, McDonald J, Wickstead B. 2019 Ndc80/Nuf2-like protein KKIP1 connects a stable kinetoplastid outer kinetochore complex to the inner kinetochore and responds to metaphase tension. *bioRxiv* 764829. (doi:10.1101/764829)
16. Black BE, Cleveland DW. 2011 Epigenetic centromere propagation and the nature of CENP-A nucleosomes. *Cell* **144**, 471–479. (doi:10.1016/j.cell.2011.02.002)
17. Wickstead B, Ersfeld K, Gull K. 2004 The small chromosomes of *Trypanosoma brucei* involved in antigenic variation are constructed around repetitive palindromes. *Genome Res.* **14**, 1014–1024. (doi:10.1101/gr.2227704)
18. Obado SO, Bot C, Nilsson D, Andersson B, Kelly JM. 2007 Repetitive DNA is associated with centromeric domains in *Trypanosoma brucei* but not *Trypanosoma cruzi*. *Genome Biol.* **8**, R37. (doi:10.1186/gb-2007-8-3-r37)
19. Echeverry MC, Bot C, Obado SO, Taylor MC, Kelly JM. 2012 Centromere-associated repeat arrays on *Trypanosoma brucei* chromosomes are much more extensive than predicted. *BMC Genomics* **13**, 29. (doi:10.1186/1471-2164-13-29)
20. Zimmermann L *et al*. 2018 A completely reimplemented MPI bioinformatics toolkit with a new HHpred server at its core. *J. Mol. Biol.* **430**, 2237–2243. (doi:10.1016/j.jmb.2017.12.007)
21. Dyda F, Klein DC, Hickman AB. 2000 GCN5-related N-acetyltransferases: a structural overview. *Annu. Rev. Biophys. Biomol. Struct.* **29**, 81–103. (doi:10.1146/annurev.biophys.29.1.81)
22. Roth SY, Denu JM, Allis CD. 2001 Histone acetyltransferases. *Annu. Rev. Biochem.* **70**, 81–120. (doi:10.1146/annurev.biochem.70.1.81)
23. Salah Ud-Din AIM, Tikhomirova A, Roujeinikova A. 2016 Structure and functional diversity of GCN5-related *N*-acetyltransferases (GNAT). *Int. J. Mol. Sci.* **17**, 1018. (doi:10.3390/ijms17071018)
24. Mo F *et al*. 2016 Acetylation of Aurora B by TIP60 ensures accurate chromosomal segregation. *Nat. Chem. Biol.* **12**, 226–232. (doi:10.1038/nchembio.2017)
25. Ohzeki J-I *et al*. 2016 KAT7/HBO1/MYST2 regulates CENP-A chromatin assembly by antagonizing Suv39h1-mediated centromere inactivation. *Dev. Cell* **37**, 413–427. (doi:10.1016/j.devcel.2016.05.006)
26. Llauró A, Hayashi H, Bailey ME, Wilson A, Ludzia P, Asbury CL, Akiyoshi B. 2018 The kinetoplastid kinetochore protein KKT4 is an unconventional microtubule tip-coupling protein. *J. Cell Biol.* **217**, 3886–3900. (doi:10.1083/jcb.201711181)
27. Zhou Q, Pham KTM, Hu H, Kurasawa Y, Li Z. 2019 A kinetochore-based ATM/ATR-independent DNA damage checkpoint maintains genomic integrity in trypanosomes. *Nucleic Acids Res.* **47**, 7973–7988. (doi:10.1093/nar/gkz476)
28. Dean S, Sunter JD, Wheeler RJ. 2017 TrypTag.org: a trypanosome genome-wide protein localisation resource. *Trends Parasitol.* **33**, 80–82. (doi:10.1016/j.pt.2016.10.009)
29. Halliday C, Billington K, Wang Z, Madden R, Dean S, Sunter JD, Wheeler RJ. 2019 Cellular landmarks of *Trypanosoma brucei* and *Leishmania mexicana*. *Mol. Biochem. Parasitol.* **230**, 24–36. (doi:10.1016/j.molbiopara.2018.12.003)
30. Ishii M, Akiyoshi B. 2019 Unconventional kinetochore kinases KKT10/19 promote the metaphase to anaphase transition in *Trypanosoma brucei*. *bioRxiv* 806224. (doi:10.1101/806224)
31. Akiyoshi B. 2016 The unconventional kinetoplastid kinetochore: from discovery toward functional understanding. *Biochem. Soc. Trans.* **44**, 1201–1217. (doi:10.1042/BST20160112)
32. Poon SK, Peacock L, Gibson W, Gull K, Kelly S. 2012 A modular and optimized single marker system for generating *Trypanosoma brucei* cell lines expressing T7 RNA polymerase and the tetracycline repressor. *Open Biol.* **2**, 110037. (doi:10.1098/rsob.110037)
33. Brun R. 1979 Cultivation and *in vitro* cloning or procyclic culture forms of *Trypanosoma brucei* in a semi-defined medium. Short communication. *Acta Trop.* **36**, 289–292.
34. Merritt C, Stuart K. 2013 Identification of essential and non-essential protein kinases by a fusion PCR method for efficient production of transgenic *Trypanosoma brucei*. *Mol. Biochem. Parasitol.* **190**, 44–49. (doi:10.1016/j.molbiopara.2013.05.002)
35. Dean S, Sunter J, Wheeler RJ, Hodkinson I, Gluenz E, Gull K. 2015 A toolkit enabling efficient, scalable and reproducible gene tagging in trypanosomatids. *Open Biol.* **5**, 140197. (doi:10.1098/rsob.140197)
36. Kelly S *et al*. 2007 Functional genomics in *Trypanosoma brucei*: a collection of vectors for the expression of tagged proteins from endogenous and ectopic gene loci. *Mol. Biochem. Parasitol.* **154**, 103–109. (doi:10.1016/j.molbiopara.2007.03.012)
37. Schneider CA, Rasband WS, Eliceiri KW. 2012 NIH Image to ImageJ: 25 years of image analysis. *Nat. Methods* **9**, 671–675. (doi:10.1038/nmeth.2089)
38. Aslett M *et al*. 2010 TriTrypDB: a functional genomic resource for the Trypanosomatidae. *Nucleic Acids Res.* **38**, D457–D462. (doi:10.1093/nar/gkp851)
39. Ericson M, Janes MA, Butter F, Mann M, Ullu E, Tschudi C. 2014 On the extent and role of the small proteome in the parasitic eukaryote *Trypanosoma brucei*. *BMC Biol.* **12**, 14. (doi:10.1186/1741-7007-12-14)
40. Parsons M, Ramasamy G, Vasconcelos EJR, Jensen BC, Myler PJ. 2015 Advancing *Trypanosoma brucei* genome annotation through ribosome profiling and spliced leader mapping. *Mol. Biochem. Parasitol.* **202**, 1–10. (doi:10.1016/j.molbiopara.2015.09.002)
41. Altschul SF, Madden TL, Schäffer AA, Zhang J, Zhang Z, Miller W, Lipman DJ. 1997 Gapped BLAST and PSI-BLAST: a new generation of protein database search programs. *Nucleic Acids Res.* **25**, 3389–3402. (doi:10.1093/nar/25.17.3389)
42. Potter SC, Luciani A, Eddy SR, Park Y, Lopez R, Finn RD. 2018 HMMER web server: 2018 update. *Nucleic Acids Res.* **46**, W200–W204. (doi:10.1093/nar/gky448)
43. Eddy SR. 1998 Profile hidden Markov models. *Bioinformatics* **14**, 755–763. (doi:10.1093/bioinformatics/14.9.755)
44. Katoh K, Standley DM. 2013 MAFFT multiple sequence alignment software version 7: improvements in performance and usability. *Mol. Biol. Evol.* **30**, 772–780. (doi:10.1093/molbev/mst010)
45. Waterhouse AM, Procter JB, Martin DMA, Clamp M, Barton GJ. 2009 Jalview Version 2–a multiple sequence alignment editor and analysis workbench. *Bioinformatics* **25**, 1189–1191. (doi:10.1093/bioinformatics/btp033)
46. Lupas A, Van Dyke M, Stock J. 1991 Predicting coiled coils from protein sequences. *Science* **252**, 1162–1164. (doi:10.1126/science.252.5009.1162)
47. El-Sayed NM *et al*. 2005 The genome sequence of *Trypanosoma cruzi*, etiologic agent of Chagas disease. *Science* **309**, 409–415. (doi:10.1126/science.1112631)

48. Ivens AC *et al*. 2005 The genome of the kinetoplastid parasite, *Leishmania major*. *Science* **309**, 436–442. (doi:10.1126/science.1112680)
49. Kraeva N *et al*. 2015 *Leptomonas seymouri*: adaptations to the dixenous life cycle analyzed by genome sequencing, transcriptome profiling and co-infection with *Leishmania donovani*. *PLoS Pathog.* **11**, e1005127. (doi:10.1371/journal.ppat.1005127)
50. Jackson AP *et al*. 2016 Kinetoplastid phylogenomics reveals the evolutionary innovations associated with the origins of parasitism. *Curr. Biol.* **26**, 161–172. (doi:10.1016/j.cub.2015.11.055)
51. Tanifuji G *et al*. 2017 Genome sequencing reveals metabolic and cellular interdependence in an amoeba-kinetoplastid symbiosis. *Sci. Rep.* **7**, 11688. (doi:10.1038/s41598-017-11866-x)
52. UniProt Consortium. 2019 UniProt: a worldwide hub of protein knowledge. *Nucleic Acids Res.* **47**, D506–D515. (doi:10.1093/nar/gky1049)